

## The Effects of Aluminum Oxide in Restructuring Iron Single Crystal Surfaces for Ammonia Synthesis

D. R. STRONGIN, S. R. BARE, AND G. A. SOMORJAI

*Materials and Molecular Research Division, Lawrence Berkeley Laboratory, and Department of Chemistry, University of California, Berkeley, California 94720*

Received July 8, 1986; revised August 26, 1986

The effect of aluminum oxide and potassium on the ammonia synthesis over the (111), (100), and (110) faces of iron has been investigated. A restructuring of the Fe(110) and Fe(100) surfaces, induced by the presence of aluminum oxide and 20 Torr of water vapor, takes place making the restructured surfaces almost as active as the clean Fe(111) plane in the ammonia synthesis reaction (20 atm reactant pressure of hydrogen and nitrogen). The high activity of the restructured surfaces is maintained for over 4 hr of ammonia synthesis. Without the presence of aluminum oxide, treatment of the Fe(110) and Fe(100) surfaces with 20 Torr of water vapor again produces restructured surfaces which are almost as active as the Fe(111) plane for a short period. However, in this case deactivation of the restructured surfaces into the respective clean, unstructured surfaces occurs within 1 hr of ammonia synthesis. Restructuring of the Fe(111) with 20 Torr of water vapor produces only a slight decrease in ammonia synthesis activity. The enhancement in rate of the restructured Fe(110) and Fe(100) surfaces, with or without aluminum oxide, might be explained by the formation of active surface orientations for ammonia synthesis (i.e., Fe(111) and Fe(211)), which contain  $C_7$  sites (iron atoms with seven nearest neighbors), during the water vapor treatments. These restructured surfaces are only stable in the ammonia synthesis conditions when aluminum oxide is present. Potassium adsorbed alone or with coadsorbed aluminum oxide exhibits no promotional effects under the water vapor pretreatment conditions used in this study. © 1987

Academic Press, Inc.

### 1. INTRODUCTION

The industrial synthesis of ammonia occurs over an iron catalyst promoted with the oxides of potassium ( $K_2O$ ), aluminum ( $Al_2O_3$ ), calcium ( $CaO$ ), and silicon ( $SiO_2$ ). The preparation of the catalyst involves the fusing of about 2% by weight of the promoters with  $Fe_3O_4$  (magnetite) followed by reduction. Over 70 years of work has gone into elucidating the effects of the potassium oxide and aluminum oxide since they are thought to represent the two different types of effects (electronic and structural promotion) exhibited by the promoters. Studies on the industrial catalyst have shown that the addition of  $Al_2O_3$  increases the surface area of the catalyst from an initial value of 1  $m^2/g$ -cat. (unpromoted iron) to a value of 25  $m^2/g$ -cat. The addition of  $K_2O$  decreases the surface area to about 10  $m^2/g$ -cat. but in-

creases the ammonia synthesis rate by a factor of 3 (1, 2). Recent surface science work (3, 4) has shown that the addition of potassium of an Fe(100) face increases the rate of dissociative nitrogen chemisorption, the rate-limiting step in the ammonia synthesis reaction (5-7), to a level equivalent to the most active Fe(111) plane.

The catalytic studies carried out on the industrial catalyst have usually been performed in systems which operate at pressures greater than 1 atmosphere (1, 6). In this type of environment the surface of the working catalyst cannot be characterized directly. Surface science studies on the adsorption of nitrogen on iron single crystals have been carried out in ultrahigh vacuum systems, where pressures do not exceed  $10^{-4}$  Torr (1 Torr = 133.3 N/m<sup>2</sup>) (3, 4) and the synthesis of ammonia does not proceed at a detectable rate. The development of

combined high-pressure/ultrahigh-vacuum systems in our laboratory bridges this pressure gap and allows the study of catalytic reaction rates and selectivity on well-characterized single crystal surfaces. Under ultrahigh vacuum an iron sample can be characterized by surface-sensitive techniques, and at high-pressure ammonia synthesis conditions (20 atm of a stoichiometric mixture of  $N_2$  and  $H_2$ ), rates of ammonia production can be determined as a function of surface composition and structure. Our studies of the ammonia synthesis on the (111), (100), and (110) crystal faces of iron revealed the marked structure sensitivity of this reaction ( $Fe(111) > Fe(100) > Fe(110)$ ) (8). Recent studies in our laboratory which included the (211) and (210) crystal faces (9), clearly implicated the unique activity of seven coordinated sites for ammonia synthesis that are only present in the (111) and (211) crystal faces to dissociate dinitrogen (the rate-limiting step for this reaction).

We report the study of the effects of promoters, aluminum oxide and potassium, on the synthesis of ammonia on single crystal iron surfaces of (111), (100), and (110) orientation. We find that a pretreatment of the iron catalyst, in the presence of aluminum oxide, using water vapor must be performed prior to the ammonia synthesis for aluminum oxide to function as a promoter. In this circumstance the rates of the reaction over the less active (110) and (100) faces increases markedly to attain the rate observed over the most active  $Fe(111)$  face. The presence of aluminum oxide helps to maintain this high activity which is caused by the restructuring of the less active crystal faces to surfaces as active as the  $Fe(111)$  or  $Fe(211)$  faces (9). Under our conditions of pretreatment and reaction reported here, potassium alone or together with aluminum oxide has no discernible effects on the catalyst activity.

## 2. EXPERIMENTAL

The experiments in this study were performed in a stainless-steel ultrahigh-vac-

uum (UHV) chamber with a base pressure less than  $2 \times 10^{-9}$  Torr. The chamber is equipped with a retarding field analyzer for low energy electron diffraction (LEED) and Auger electron spectroscopy (AES) and with a hydraulically operated high-pressure cell which constitutes part of a microbatch reactor. A mass spectrometer is used to monitor residual gases in the chamber and to perform temperature programmed desorption (TPD). The ionizer on the mass spectrometer is enclosed by a gold-plated tube with an opening (0.25 cm diameter) at the end. This whole assembly was mounted on a bellows so that during TPD experiments the aperture could be brought close to a face of the sample. This procedure improved sensitivity and eliminated the detection of gases desorbing from the support wires.

A typical reaction sequence would occur as follows. The sample is prepared and characterized in UHV by LEED and AES and is enclosed by the high-pressure cell to form an external reaction loop. The loop is then pressurized with the reactant gases (20 atm of 3:1 mixture of  $H_2$  and  $N_2$ ) which are circulated by a positive displacement pump, and the sample is heated to the reaction temperature (all ammonia synthesis reactions were run at 673 K unless otherwise noted). Ammonia formation is monitored by periodically taking samples from the reaction loop and passing the samples through a photoionization detector (PID) sensitive only to the partial pressure of ammonia. After reaction the crystal is cooled to 373 K, in the reaction mixture, and the reactant gases are then evacuated from the cell. The sample is returned to the UHV environment where AES, LEED, and TPD are performed.

Water vapor treatment of the iron surfaces was performed by enclosing the sample in the high-pressure cell and then equilibrating the desired pressure of water vapor within the external loop. All the treatments were carried out at 723 K for 30 min (only the pressure of water vapor will be used to

describe the treatments mentioned throughout the text).

The single crystal samples used were on the average 1-cm<sup>2</sup> disks about 1 mm thick. They were cut and polished by standard metallurgical techniques. The sample was spot-welded between 0.25-mm-diameter platinum wire. The crystal was heated resistively and its temperature was monitored with a Chromel–Alumel thermocouple spot-welded to the edge of the sample. The major impurities in the iron single crystals were sulfur and carbon. The sulfur was removed by prolonged argon ion sputtering ( $4\text{--}5 \times 10^{-6}$  A/cm<sup>2</sup>) while the sample was held at 873 K. Carbon was removed by treating the crystal with  $1 \times 10^{-7}$  Torr of oxygen while sputtering.

A Knudsen cell was used for the evaporation of aluminum. The aluminum was oxidized to Al<sub>x</sub>O<sub>y</sub> (aluminum oxide will be denoted as Al<sub>x</sub>O<sub>y</sub> due to the uncertainty in the aluminum and oxygen stoichiometry) by heating the surface to 673 K under  $5 \times 10^{-8}$  Torr of water. The extent of aluminum oxidation was verified by the shift of the 67-eV aluminum LVV Auger peak to 54 eV, representative of bulk Al<sub>2</sub>O<sub>3</sub> (10). Coverages of Al<sub>x</sub>O<sub>y</sub> were determined by titrating the surface with <sup>13</sup>CO. Since CO chemisorbs on iron and not Al<sub>2</sub>O<sub>3</sub> (11) the relative amount of free iron surface could be calculated by taking the difference in integral areas between CO/Fe and CO/Al<sub>x</sub>O<sub>y</sub>/Fe TPD peaks. Rates of ammonia synthesis reported throughout this paper were determined by taking into account the amount of free iron surface on each crystal. Coverages above 1 monolayer (ML) were estimated by dividing the evaporation time by the time it took to evaporate 1 monolayer of Al<sub>x</sub>O<sub>y</sub> (defined as the point where no CO chemisorbs to the sample). It is proposed later in this paper (see Section 3.1) that Al<sub>x</sub>O<sub>y</sub> grows in three-dimensional islands on the iron surface; thus, the point where CO can no longer chemisorb on the sample might actually correspond to more than one atomic layer. The ratio of intensities of the 47-eV iron

and 54-eV Al<sub>x</sub>O<sub>y</sub> Auger peaks were calibrated against the CO titration data so that coverages of aluminum oxide could alternatively be determined by AES. Potassium was deposited onto the single crystals by a Saes Getters source. The potassium coverage was determined from uptake curves where the intensity of the 252-eV potassium Auger peak was plotted against dose time (the evaporation rate was constant in these experiments).

The reactant gases (N<sub>2</sub> and H<sub>2</sub>) were research purity. They were further purified by passage through a molecular sieve trap and a liquid nitrogen-cooled coil. The distilled water used in this study was outgassed by repeated freeze–thaw cycles.

Iron samples were examined by scanning electron microscopy (SEM) after removal from the UHV chamber. Transfer in air to the microscope did not seem to alter the sample surfaces because identical micrographs were seen for samples after exposure to air for 1 day or 1 week.

### 3. RESULTS

#### 3.1. Auger Electron Spectroscopy and Low-Energy Electron Diffraction Studies

The growth of oxidized aluminum on the iron single crystals was studied by AES and LEED. There was no indication of any long-range ordering of the Al<sub>x</sub>O<sub>y</sub> at any coverage on the Fe(111), Fe(100), and Fe(110) planes. Using AES, the 54-eV aluminum oxide transition intensity was plotted against the iron 47- and 652-eV peak intensities. In both cases no breaks in the curves were found, indicating three-dimensional Al<sub>x</sub>O<sub>y</sub> island growth (12).

AES was used to estimate the coverage of Al<sub>x</sub>O<sub>y</sub> in the near-surface region on the three different iron surfaces used in this study before and after the various water vapor treatments. On both the Fe(110) and Fe(111) surfaces an initial concentration of 2 monolayers of Al<sub>x</sub>O<sub>y</sub> decreases to about 50% of a monolayer after being treated with

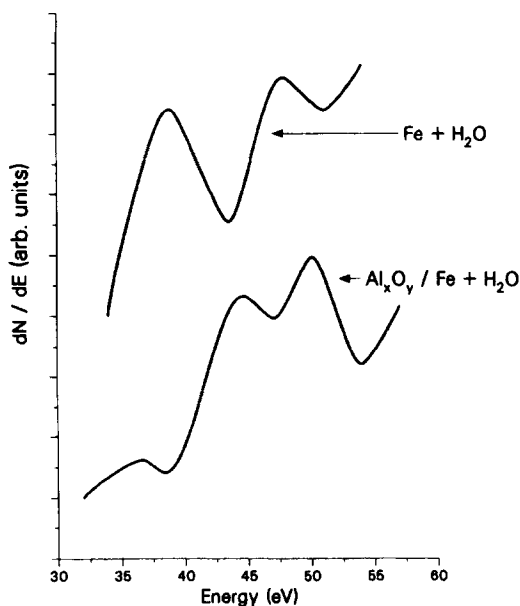


FIG. 1. AES spectra of oxidized iron and a partially oxidized iron-aluminum oxide surface. Note the shift of the 42 eV iron peak to 39 eV when aluminum oxide is coadsorbed on the oxidized surface.

0.05 Torr of water vapor and subsequent reduction in the  $H_2$  and  $N_2$  synthesis gas mixture. A more drastic reduction in the  $Al_xO_y$  coverage was observed if the sample was treated with 0.4 Torr of water. In this case the  $Al_xO_y$  was barely detectable by AES (about 5% of a monolayer). Argon ion sputtering the surface ( $4-5 \times 10^{-6}$  A/cm<sup>2</sup>) at room temperature uncovered additional  $Al_xO_y$ . Sputtering the sample at 823 K revealed less  $Al_xO_y$  due to the diffusion of the  $Al_xO_y$  into the bulk or iron on top of the  $Al_xO_y$ . Prolonged sputtering at 823 K eventually caused the (1 × 1) LEED pattern to appear on both the Fe(111) and Fe(110) surfaces.

The behavior of  $Al_xO_y$  on the Fe(100) face is different than that on the (110) and (111) planes. After a treatment with 0.05 or 0.4 Torr of water vapor the ratio of the aluminum Auger signal to the iron signal was unchanged, indicating that no  $Al_xO_y$  had left the surface. After a 20-Torr treatment of water vapor, about 50% of a monolayer

of  $Al_xO_y$  is left on the  $Al_xO_y/Fe(100)$  surface.

Auger peak positions were used to study the cooperative interaction between  $Al_xO_y$  and iron in the presence of water vapor because the energy of an Auger transition of an element is often sensitive to the chemical environment (13). Metallic iron has an MVV Auger transition at 47 eV which splits into a 42- and 52-eV doublet in the oxide (the 42-eV peak has been attributed to the participation of oxygen 2p electrons and the 52-eV Auger peak to the influence of iron d electrons) (14). Elemental aluminum exhibits a LVV Auger peak at 68 eV which shifts to 54 eV in the oxide (10). When  $Al_xO_y$  is deposited on the iron substrate only 47- and 54-eV peaks are present. When the  $Al_xO_y/Fe$  surface is treated with water vapor the 42-eV peak, representative of iron oxide, shifts to 39 eV (Fig. 1), possibly indicating an alteration in the iron-oxygen bond and a chemical interaction between  $Al_xO_y$  and iron in an oxidizing environment (i.e.,  $Fe + Al_2O_3 + H_2O = FeAl_2O_4 + H_2$ ).

### 3.2. Reaction Rate Studies

The initial rate of ammonia synthesis was determined over the clean Fe(111), Fe(100), and Fe(110) surfaces (Fig. 2). The addition of aluminum oxide alone, elemental potassium coadsorbed with oxygen and aluminum oxide, or potassium coadsorbed with aluminum oxide on the (110), (100), and (111) faces of iron decreases the rate of ammonia synthesis in direct proportion to the amount of surface covered by the additive, in agreement with work that has been reported recently (15). Rates of ammonia synthesis were also obtained over these different surfaces after they had been pretreated with water vapor.

*3.2.1. Clean iron single crystals treated with water vapor prior to the ammonia synthesis reaction.* Treatment of the clean (110), (100), and (111) surfaces with water vapor pressures of 0.05 or 0.4 Torr produces heavily oxidized surfaces as shown

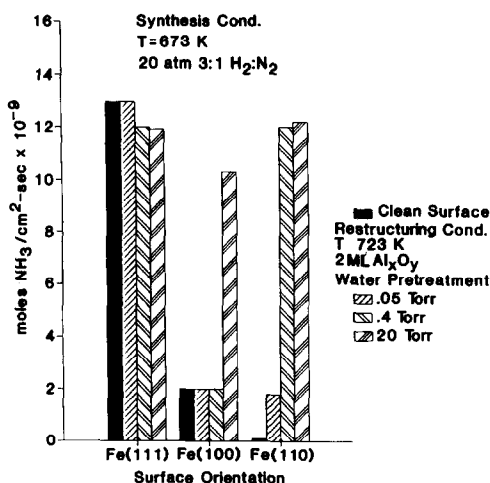


FIG. 2. Ammonia synthesis rates over clean iron single crystals and restructured Al<sub>x</sub>O<sub>y</sub>/Fe surfaces. A rate is given to the clean Fe(110) surface in this figure for clarity but in actuality the ammonia yield from this crystal face is below the detection limit of the PID ( $1 \times 10^{-10}$  mole NH<sub>3</sub>/cm<sup>2</sup>-sec) used in this study.

by the splitting of the 47-eV MVV iron Auger peak into 42- and 52-eV peaks (14). The oxidized surfaces are readily reduced under the conditions used for the ammonia synthesis reaction, and the respective Fe(110), Fe(100), and Fe(111) surfaces are regenerated.

Treatment of a clean Fe(110) surface with 20 Torr of water vapor followed by reduction under synthesis conditions leaves a restructured surface (no  $(1 \times 1)$  LEED pattern is obtained) whose *initial* ammonia synthesis activity is close to that of the (111) plane of iron. Visual inspection of the crystal shows that the initial mirror finish of the crystal is lost and a dull luster is now apparent. If this surface is kept under ammonia synthesis conditions for 1 hr the surface again becomes inactive (Fig. 3) and a  $(1 \times 1)$  LEED pattern representative of the Fe(110) surface appears.

A 20-Torr water vapor pretreatment also restructures the (111) and (100) planes of iron. The restructured Fe(111) surface (broad and diffuse  $(1 \times 1)$  LEED spots are obtained) shows a small decrease (about 5%) in its ammonia synthesis activity. The

restructured Fe(100) plane (no LEED pattern is obtained) becomes almost as active as the (111) face of iron. Like the restructured Fe(110) face the activity of the restructured (111) and (100) surfaces return to their respective clean surface activity after 1 hr of ammonia synthesis. Sharp  $(1 \times 1)$  LEED patterns for both surfaces are observed at this time.

3.2.2. Al<sub>x</sub>O<sub>y</sub>/Fe surfaces pretreated in water vapor prior to the ammonia synthesis reaction. Treatment of Al<sub>x</sub>O<sub>y</sub> (0.5–1.5 monolayers)/Fe surfaces with 0.05 and 0.4 Torr of water vapor produced no restructuring as judged by the ammonia synthesis rate on the (111), (100), and (110) faces of iron.

Major changes in the activity of ammonia production for the Fe(110) face occur when 2 or more monolayers of Al<sub>x</sub>O<sub>y</sub> are deposited on the surface prior to the water vapor treatment. After a water vapor treatment of 0.05 Torr, the Al<sub>x</sub>O<sub>y</sub>/Fe(110) surface restructures. The restructured surface is now about as active as the Fe(100) plane (Fig. 2). If 2 monolayers of Al<sub>x</sub>O<sub>y</sub> are

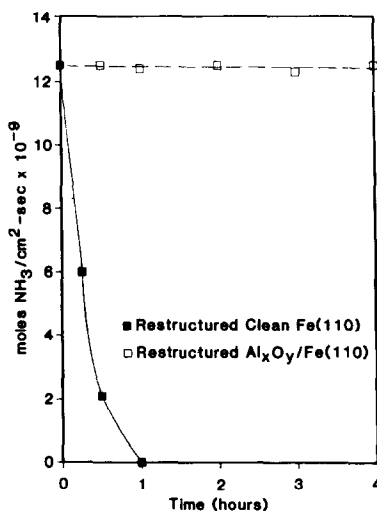


FIG. 3. The effect of Al<sub>x</sub>O<sub>y</sub> on the activity of the restructured Fe(110) surface under the ammonia synthesis conditions. Deactivation of the clean restructured Fe(110) surface occurs within 1 hr. The restructured Al<sub>x</sub>O<sub>y</sub>/Fe(110) surface maintains its activity for more than 4 hr.

on a new Fe(110) surface then exposure to 0.4 or 20 Torr of water vapor produces a restructured surface almost as active as the Fe(111) crystal face (Fig. 2). The restructured  $\text{Al}_x\text{O}_y/\text{Fe}(110)$  surface retains its high ammonia synthesis activity longer than 4 hr under ammonia synthesis conditions (Fig. 3).

An Fe(111) surface with 2 monolayers of  $\text{Al}_x\text{O}_y$  shows no noticeable change in activity when pretreated with 0.05 Torr of water vapor. Exposure to 0.4 or 20 Torr of water vapor restructures the surface, producing a slight decrease (about 5%) in ammonia synthesis activity (Fig. 2).

The  $\text{Al}_x\text{O}_y/\text{Fe}(100)$  surface exhibited no restructuring when exposed to 0.05 or 0.4 Torr of water vapor, conditions which restructured the  $\text{Al}_x\text{O}_y/\text{Fe}(110)$  and  $\text{Al}_x\text{O}_y/\text{Fe}(111)$  surfaces. Treatment of the  $\text{Al}_x\text{O}_y/\text{Fe}(110)$  surface with 20 Torr of water vapor caused restructuring and enhanced activity for the ammonia synthesis reaction. The synthesis rate over the restructured  $\text{Al}_x\text{O}_y/\text{Fe}(100)$  surface was similar to the clean Fe(111) surface activity (Fig. 2). No deactivation was observed for the restructured  $\text{Al}_x\text{O}_y/\text{Fe}(100)$  surface after 4 hr of ammonia synthesis.

All the restructured  $\text{Al}_x\text{O}_y/\text{Fe}$  surfaces maintained their activity even after any surface  $\text{Al}_x\text{O}_y$  had been removed by ion sputtering as monitored by AES. A  $^{13}\text{C}$ O titration could not be used to determine the  $\text{Al}_x\text{O}_y$  coverage in that all the restructured surfaces (after the surface  $\text{Al}_x\text{O}_y$  had been removed by argon ion sputtering) chemisorbed substantially less carbon monoxide than the respective clean, unrestructured surfaces. For example, the restructured Fe(110) and Fe(100) surfaces chemisorbed approximately 40% less CO than the clean Fe(110) and Fe(100) faces, respectively. Prolonged sputtering (2–4 hr at 823 K) caused the restructured surfaces to exhibit ( $1 \times 1$ ) LEED patterns and ammonia synthesis activities representative of the clean, unrestructured surfaces (no  $\text{Al}_x\text{O}_y$  was present at this time as judged by AES).

*3.2.3. Water vapor pretreatment of clean and  $\text{Al}_x\text{O}_y/\text{Fe}$  single crystal surfaces in the presence of coadsorbed potassium.* Coverages of 0.1 to 1.0 monolayer of potassium adsorbed alone on the (111), (100), and (110) faces of iron failed to produce any promotional effects after pretreatments with 0.05, 0.4, and 20 Torr of water vapor (after the water vapor treatments the coverage of potassium was never more than 0.4 monolayer and it did not exceed 0.1 monolayer after the ammonia synthesis reaction, in agreement with previous work (15)).

The same coverages of potassium coadsorbed with 2 monolayers of aluminum oxide on the Fe(110), Fe(100), and Fe(111) surfaces hindered the restructuring process in water vapor. As increasing amounts of potassium were coadsorbed more aluminum oxide was detected by AES after water pretreatments of 20 Torr and less restructuring of the iron occurred (rates of ammonia synthesis over these surfaces were less than those surfaces which were restructured with just aluminum oxide). There was an one-to-one ratio between aluminum oxide and potassium on the surface (15) and in an extreme case where 1 monolayer of potassium was deposited on 2 monolayers of aluminum oxide, AES showed that no aluminum oxide or potassium left the iron surface after a 20-Torr water vapor pretreatment and restructuring failed to occur.

*3.2.4. Activation energy for the ammonia synthesis reaction over clean and restructured iron.* The initial rate of ammonia synthesis was determined for the restructured  $\text{Al}_x\text{O}_y/\text{Fe}(110)$  and restructured clean Fe(110) surfaces at every 25 K interval between 673 and 823 K. Using an Arrhenius plot, the apparent activation energy of both restructured surfaces was found to be  $18.6 \pm 1$  kcal/mole, in close agreement with the value of  $19.4 \pm 0.5$  kcal/mole obtained for the clean single crystal surfaces (8).

### 3.3. Surface Structure Characterization

The synthesis of ammonia from its elements is a structure-sensitive reaction over

iron, and variation of rates observed in this study due to the pretreatments suggests that new surface orientations are being created. In an attempt to characterize the structure of the new surfaces scanning electron microscopy and temperature programmed desorption were performed on the clean and restructured surfaces. SEM gave information on the microscopic appearance of the surfaces while TPD gave insight into the nature of the crystal orientations present on the restructured surfaces.

*3.3.1. Scanning electron microscopy.* The development of a clean Fe(110) single crystal surface into a restructured surface was followed by SEM. Figure 4 shows micrographs taken of restructured Al<sub>x</sub>O<sub>y</sub>/Fe(110) surfaces (a clean, unrestructured iron single crystal showed only a flat, featureless surface). At an exposure of 0.05 Torr of water vapor the formation of crystallites, about 1 μm in diameter, appear on the Al<sub>x</sub>O<sub>y</sub>/Fe(110) surface (Fig. 4a). Using 0.4 Torr of water vapor reconstructs the entire surface as can be seen in Fig. 4b.

An Fe(110) surface restructured under 20 Torr of water vapor is shown in Fig. 5a. The surface appears uniform in appearance, unlike the Al<sub>x</sub>O<sub>y</sub>/Fe(110) restructured surface. Figure 5b shows the same surface after 1 hr of ammonia synthesis. The surface now shows less pronounced features, similar to the unrestructured Fe(110) plane. This is supported by the appearance of a (1 × 1) Fe(110) LEED pattern and inactivity toward the production of ammonia in the synthesis reaction.

*3.3.2. Temperature programmed desorption.* Ammonia adsorption and desorption on the Fe(111), Fe(100), and Fe(110) surfaces have been studied under UHV (16, 17). Molecular ammonia completely desorbs from all the iron surfaces by 400 K. In contrast to this it has been found in this study that after the high-pressure ammonia synthesis reaction ammonia desorbs in the 400–750 K temperature range from all the iron single crystal surfaces studied. The mechanism has not been studied in detail

but more important to this work is that the ammonia desorption can be used to probe the different surface orientations since different TPD spectra are observed following ammonia synthesis for the (110), (100), (111), and (211) iron single crystal surfaces. The Fe(211) TPD spectrum is included because it helps support a conclusion presented later (see Section 4).

Ammonia TPD spectra for the four surfaces are shown in Fig. 6. The Fe(110) surface displays one desorption peak ( $\beta_3$ ) with a peak maximum at 658 K. Two desorption peaks are seen for the Fe(100) surface ( $\beta_2$  and  $\beta_3$ ) at 556 and 661 K. The Fe(111) surface exhibits three desorption peaks ( $\beta_1$ ,  $\beta_2$ , and  $\beta_3$ ) with peak maxima at 495, 568, and 676 K, and the Fe(211) plane has two desorption peaks ( $\beta_2$  and  $\beta_3$ ) at 570 and 676 K. Temperature programmed desorption spectra for the Al<sub>x</sub>O<sub>y</sub>/Fe(110), Al<sub>x</sub>O<sub>y</sub>/Fe(100), and Al<sub>x</sub>O<sub>y</sub>/Fe(111) surfaces restructured under 20 Torr of water vapor are shown in Fig. 7. A new desorption peak,  $\beta_2$ , develops on the restructured Al<sub>x</sub>O<sub>y</sub>/Fe(110) surface and an increase in the  $\beta_2$  peak occurs on the restructured Al<sub>x</sub>O<sub>y</sub>/Fe(100) surface. The  $\beta_2$  peaks from the restructured Al<sub>x</sub>O<sub>y</sub>/Fe(110) and Al<sub>x</sub>O<sub>y</sub>/Fe(100) surfaces grow in the same temperature range as the Fe(111) and Fe(211)  $\beta_2$  peaks. Deactivation of the restructured surfaces by prolonged sputtering at 832 K reduces the intensity of the  $\beta_2$  peaks on the restructured Al<sub>x</sub>O<sub>y</sub>/Fe(110) and Al<sub>x</sub>O<sub>y</sub>/Fe(100) surfaces to the same level as the respective clean surfaces.

The clean Fe(110), Fe(100), and Fe(111) surfaces restructured with 20 Torr of water vapor produce the same TPD spectra as the Al<sub>x</sub>O<sub>y</sub> restructured surfaces. Deactivation of the (100) and (110) clean restructured iron surfaces is quick under the ammonia synthesis conditions and the  $\beta_2$  peaks become equivalent in intensity to those of the respective clean surfaces within 1 hr of ammonia synthesis.

#### DISCUSSION

Examination of the results reveal sev-

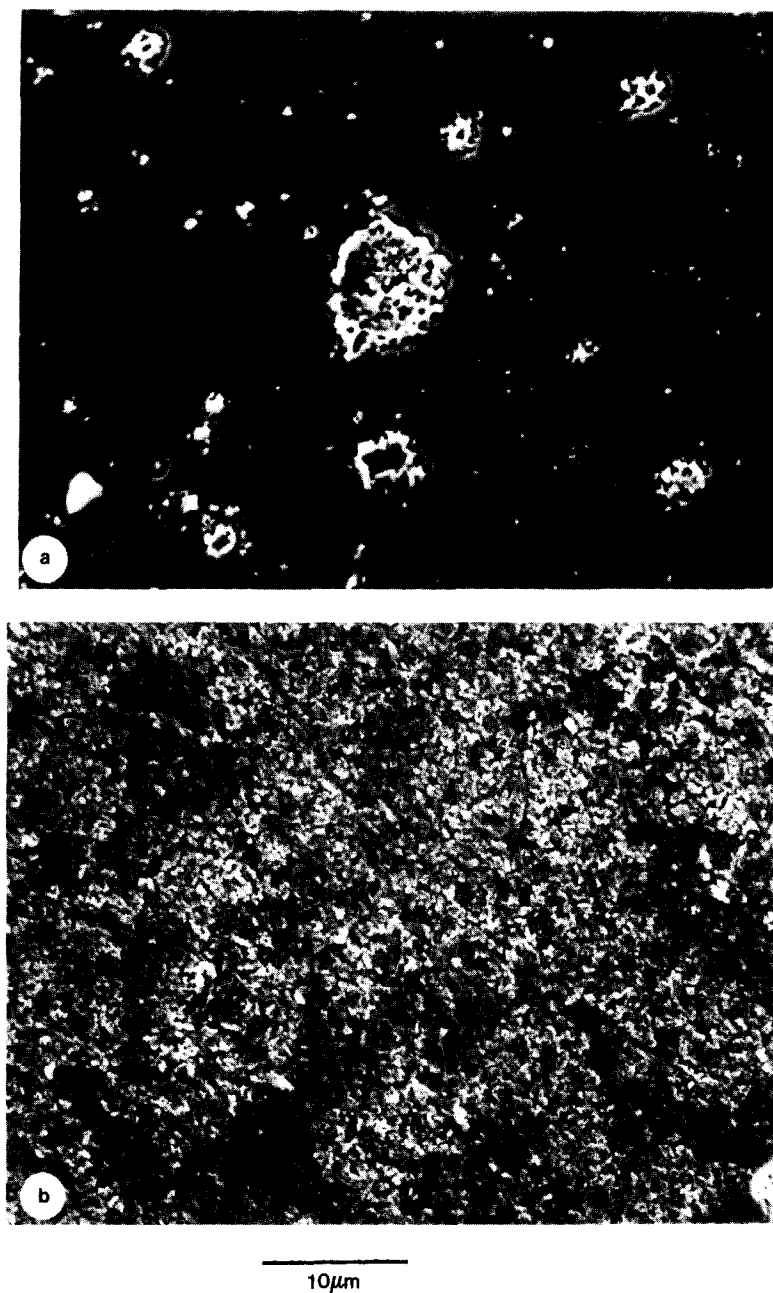


FIG. 4. SEM of the restructured  $\text{Al}_x\text{O}_y/\text{Fe}(110)$  surface. (a) An  $\text{Al}_x\text{O}_y/\text{Fe}(110)$  surface after a 0.05-Torr treatment of water vapor and subsequent reduction in the synthesis gas mixture. (b) An  $\text{Al}_x\text{O}_y/\text{Fe}(110)$  surface after a 0.4-Torr treatment of water vapor followed by reduction. The AES and SEM results indicate that aluminum oxide is located under the active iron surface during ammonia synthesis, thereby avoiding blocking of the active catalytic iron sites.

eral effects of  $\text{Al}_x\text{O}_y$  on iron single crystal surfaces in the presence of water vapor. Perhaps the most significant is that  $\text{Al}_x\text{O}_y$

prevents the reconversion of the restructured, active surfaces to ones less active in the ammonia synthesis (i.e.,  $\text{Fe}(110)$  and



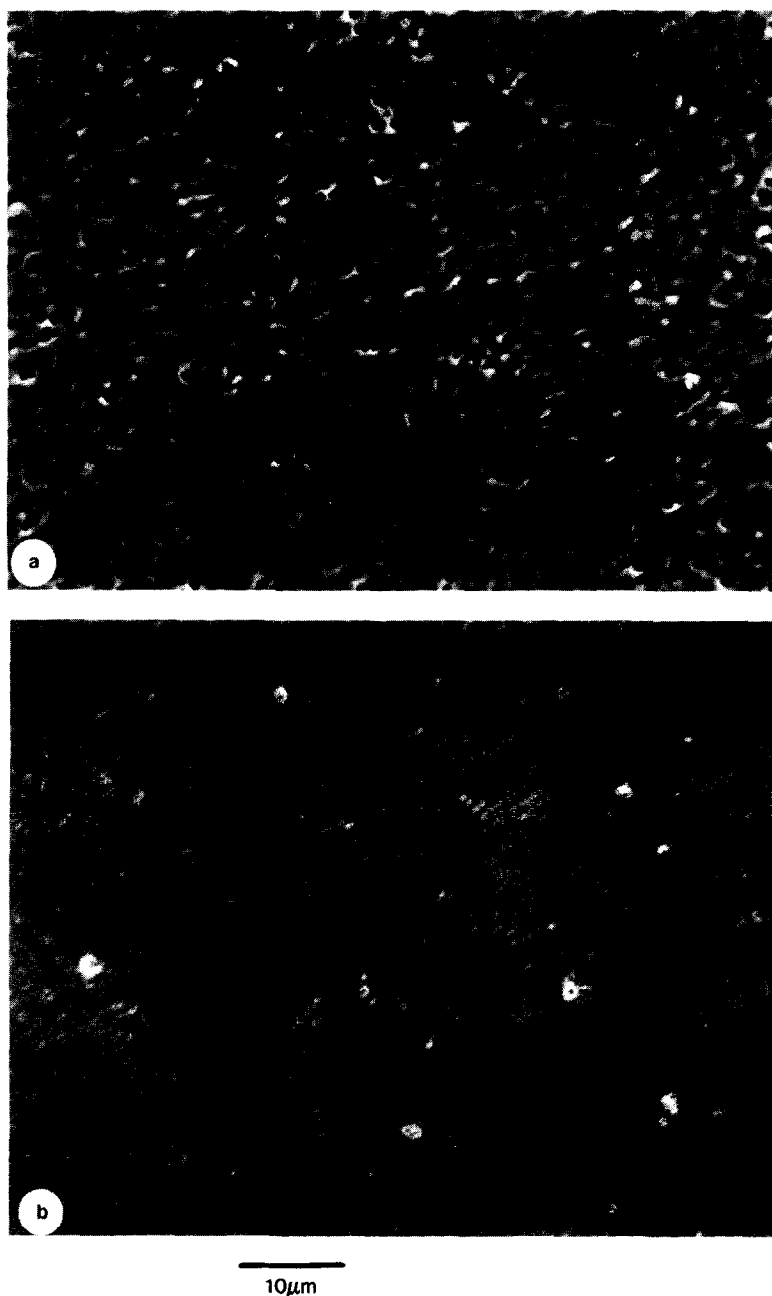


FIG. 5. SEM micrographs of the restructured Fe(110) surface (a) taken after a 20-Torr treatment of water vapor or (b) after 1 hr of ammonia synthesis (note the smoothing out of the features which were observed after the initial restructuring). The features on these surfaces are much more uniform in appearance than those on the restructured  $\text{Al}_x\text{O}_y/\text{Fe}$  surfaces.

Fe(100) surfaces). Another effect of  $\text{Al}_x\text{O}_y$  is its ability to restructure iron single crystals to new surface orientations active in the ammonia synthesis at water vapor pres-

ures lower than those needed to restructure clean iron single crystal surfaces. Since the activation energy for ammonia synthesis over the restructured  $\text{Al}_x\text{O}_y/\text{Fe}$

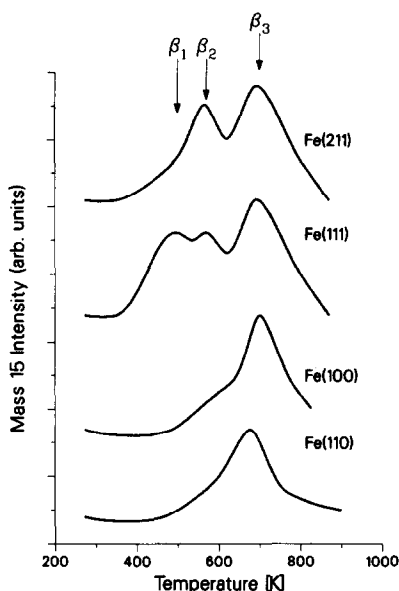


FIG. 6. Ammonia TPD from clean iron single crystals (heating rate is 10 K/sec). Different TPD spectra are found for each surface. Only the Fe(111) and Fe(211) planes exhibit large desorption peaks in the temperature range 400–600 K. These peaks are attributed to the presence of  $C_7$  sites on the (111) and (211) planes of iron.

surfaces is the same as that over the clean surface implies that iron is still the active phase for the synthesis of ammonia.

The nature of restructuring of the  $Al_xO_y/Fe$  surfaces is indicated by the kinetic and TPD results. Kinetic data show that through restructuring the activity toward ammonia synthesis of the Fe(110) and Fe(100) planes approaches that of the clean Fe(111) or Fe(211) planes while the Fe(111) plane is not affected greatly by restructuring. The activity of the clean Fe(111) and Fe(211) planes is usually attributed to the presence of  $C_7$  sites (Fe atoms with the seven nearest neighbors) (8, 9, 18). The clean Fe(100) and Fe(110) planes lack these sites. This suggests that restructuring in water vapor produces highly coordinated  $C_7$  sites on the restructured Fe(110) and Fe(100) surfaces. The increase in rates over the restructured Fe(110) and Fe(100) planes is not attributable to an increase in surface

area since less CO is adsorbed on these surfaces compared to the respective clean surfaces. A similar decrease in CO adsorption has also been observed on iron ammonia synthesis catalysts that have been restructured with ammonia (18). These results were interpreted as due to the formation of  $C_7$  sites which are not able to adsorb as much CO as lower coordinated sites because of steric reasons. This explanation is applicable to the present study and it further supports the idea of formation of  $C_7$  sites upon water vapor restructuring.

While the ammonia TPD results are not as convincing as the kinetic data, they certainly point toward the formation of surface orientations that contain  $C_7$  sites during restructuring. The growth of the  $\beta_2$  peaks upon restructuring of the Fe(110) and Fe(100) surfaces suggests that the surfaces change orientation upon water vapor treatment. The  $\beta_2$  peaks also reside in the same

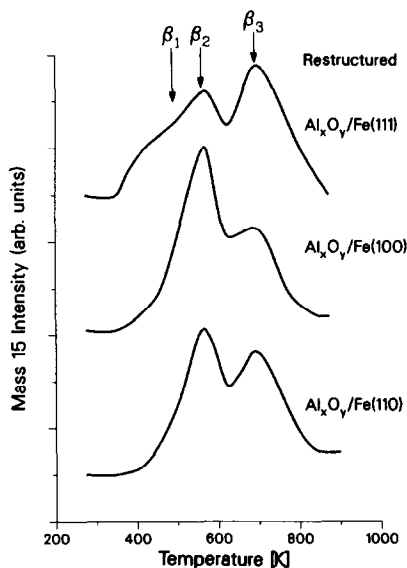


FIG. 7. Ammonia TPD from restructured iron single crystals (heating rate is 10 K/sec). A  $\beta_2$  state grows on the restructured  $Al_xO_y/Fe(110)$  surface and the restructured  $Al_xO_y/Fe(100)$  face in the same temperature range as the Fe(111)  $\beta_2$  peak and the Fe(211)  $\beta_2$  peak. This indicates that active planes for ammonia synthesis, containing  $C_7$  sites (i.e., Fe(111) and Fe(211) surfaces), are forming upon the water vapor-induced restructured surfaces.

temperature range as the Fe(111)  $\beta_2$  peak. It seems likely that the TPD peaks in this temperature range act as a signature for the C<sub>7</sub> sites since the Fe(211) surface (Fig. 6), which contains C<sub>7</sub> sites and is highly active in the ammonia synthesis reaction (9), also exhibits a  $\beta_2$  peak after the ammonia synthesis with a peak maximum at 570 K. These results suggest that surface orientations which contain C<sub>7</sub> sites, such as the Fe(111) and Fe(211) planes, are being formed during the reconstruction of clean and Al<sub>x</sub>O<sub>y</sub>-treated iron surfaces but only in the presence of Al<sub>x</sub>O<sub>y</sub> does the active restructured surface remain stable under the ammonia synthesis conditions.

The process by which iron restructures seems to involve both oxidation and reduction. Initial oxidation by water vapor destroys the original morphology of the iron surface. On reduction with synthesis gas the oxygen is removed and the resulting metallic iron is left in orientations (i.e., Fe(111) and Fe(211)) active for the ammonia synthesis. If no support phase is present (i.e., Al<sub>x</sub>O<sub>y</sub>) reconversion of the iron into less active orientations is rapid under ammonia synthesis conditions. It has been shown under UHV (19, 20) that the oxidative process on the Fe(110) plane is more facile than on the Fe(100) surface and this agrees with the fact that the Fe(110) surface can restructure, in this study, at lower water vapor pressures than are needed for the Fe(100) plane.

With the addition of Al<sub>x</sub>O<sub>y</sub> the mobility of the iron is increased and restructuring can occur at a lower pressure of water vapor. The SEM micrographs suggest that iron is forming crystallites on top of the restructured Al<sub>x</sub>O<sub>y</sub>/Fe(110) surface (opposed to the uniform appearance of the restructured clean Fe(110) surface). AES finds little Al<sub>x</sub>O<sub>y</sub> on the surface, suggesting that the iron has diffused on top of the Al<sub>x</sub>O<sub>y</sub> islands. These findings can be explained by considering wetting properties and the minimization of the free energy for the iron-aluminum oxide system.

Under vacuum or in a reducing environment (i.e., ammonia synthesis conditions), metallic iron will not spread over aluminum oxide (metallic iron has a higher surface tension than aluminum oxide (21)). Conversely, in an oxidizing environment (i.e., the water vapor treatments) iron oxide forms (the surface tension of the oxide will be lower than that of the metal (21, 22)) and a chemical interaction between iron and aluminum oxide might result, as inferred from the AES results. Both these considerations favor iron wetting the aluminum oxide. Using transmission electron microscopy it has been shown that iron wets alumina (Al<sub>2</sub>O<sub>3</sub>) in an oxidizing environment or even in the presence of hydrogen which contains trace amounts of water vapor (23). Using microelectron diffraction the formation of iron aluminate (i.e., FeAl<sub>2</sub>O<sub>4</sub>) in the presence of an oxygen source was also postulated (23).

Whereas 20 Torr of water vapor was needed to restructure clean iron single crystals, only 0.4 Torr of water vapor is needed to restructure an Al<sub>x</sub>O<sub>y</sub>/Fe surface since Al<sub>x</sub>O<sub>y</sub> provides an alternate and apparently more facile mechanism for the migration of iron. Upon reduction metallic iron is left in a highly active orientation (i.e., Fe(111) and Fe(211)) for the ammonia synthesis reaction. The Al<sub>x</sub>O<sub>y</sub> now stabilizes the active iron since if the Al<sub>x</sub>O<sub>y</sub> were not present the iron would move to positions coincident with the bulk periodicity.

The formation of an iron aluminate during reconstruction of the iron surface may be responsible for the stability of the restructured Al<sub>x</sub>O<sub>y</sub>/Fe surfaces. The formation of iron aluminate has been postulated in XPS studies on Fe/Al<sub>2</sub>O<sub>3</sub> and Fe<sub>3</sub>O<sub>4</sub>/Al<sub>2</sub>O<sub>3</sub> systems (24, 25) as well as in numerous studies on the industrial ammonia synthesis catalyst (26–28). The volume of an FeAl<sub>2</sub>O<sub>4</sub> molecule is approximately equal to the volume of seven iron atoms in a *bcc* lattice (26) so that FeAl<sub>2</sub>O<sub>4</sub> can exist as a skeleton in the iron lattice with little distortion. The low coverage of Al<sub>x</sub>O<sub>y</sub> on the re-

structured surfaces suggests that the support effect might be coming through inclusions of  $\text{FeAl}_2\text{O}_4$  in the near-surface region. This is supported by the fact that ion sputtering the restructured surfaces reveals subsurface  $\text{Al}_x\text{O}_y$ .

A promoter effect by potassium still has not been observed on iron single crystal studies which have approached industrial conditions of 100 atm total reactant pressure. Previous work reported recently (15) observed no electronic promotion when potassium was adsorbed alone or coadsorbed with oxygen and  $\text{Al}_x\text{O}_y$  on the iron surfaces. The conditions used in this study revealed no promotional effects by potassium.

Potassium promotion seems to be extremely sensitive to the environment. UHV studies (3, 4) showed that potassium increased the rate of dissociative nitrogen chemisorption by more than an order of magnitude over single crystals and polycrystalline foils but with the addition of oxygen the promotional effect decreased rapidly. The turnover numbers for unpromoted, singly promoted ( $\text{Al}_2\text{O}_3$ ), and doubly promoted ( $\text{K}_2\text{O}$  and  $\text{Al}_2\text{O}_3$ ) iron catalysts have been found to be roughly equivalent when a total pressure of 1 atm of  $\text{H}_2$  and  $\text{N}_2$  is used for the ammonia synthesis conditions (29). The studies performed in this laboratory find no electronic or structural promotion by potassium at 20 atm of 3:1  $\text{H}_2$  and  $\text{N}_2$ . To understand the effect of potassium it seems necessary to reach the industrial synthesis conditions (100 atm total pressure). Combined UHV/high pressure experiments capable of reaching these conditions are being planned for the future.

#### SUMMARY

Treating the (110), (100), and (111) faces of iron with 20 Torr of water vapor causes surface restructuring. The restructured Fe(110) and Fe(100) surfaces become as active as the clean Fe(111) surface in the ammonia synthesis. The restructured Fe(111) exhibits a slight decrease (about 5%) in activity when compared to the clean Fe(111) surface. The restructured (110), (100), and

(111) surfaces revert to their unrestructured orientations within 1 hr of ammonia synthesis.

The same restructuring on the Fe(110), Fe(100), and Fe(111) surfaces can be performed with water vapor in the presence of aluminum oxide. In this case 20 Torr of water vapor restructures the  $\text{Al}_x\text{O}_y/\text{Fe}(100)$  and only 0.4 Torr of water vapor is needed to restructure the  $\text{Al}_x\text{O}_y/\text{Fe}(110)$  surface so that they become as active as the Fe(111) face in ammonia synthesis. The restructured  $\text{Al}_x\text{O}_y/\text{Fe}(110)$  and  $\text{Al}_x\text{O}_y/\text{Fe}(100)$  surfaces maintain their activity for longer than 4 hr in the ammonia synthesis conditions. The formation of iron aluminate in the iron near-surface region is invoked to explain the stability of the restructured  $\text{Al}_x\text{O}_y/\text{Fe}$  surfaces.

The reaction rate studies and ammonia temperature programmed desorption results suggest that planes containing  $C_7$  sites, such as the Fe(211) and Fe(111) surfaces, are being created during the water vapor pretreatments with or without aluminum oxide. Only when aluminum oxide is present do these active surfaces remain stable and do not revert to less active surfaces (i.e., Fe(110) and Fe(100) planes).

Coadsorbing potassium with aluminum oxide or depositing potassium alone on iron single crystals produces no promotional effects under the water vapor pretreatments used in this study.

#### ACKNOWLEDGMENT

This work was supported by the Director, Office of Energy Research, Office of Basic Energy Sciences, Materials Science Division of the U.S. Department of Energy under Contract DE-AC03-76SF00098.

#### REFERENCES

1. Nielsen, A., "An Investigation on promoted Iron Catalysts for the Synthesis of Ammonia", Jul. Gjellerups Forlag, 3rd ed., Copenhagen (1968).
2. Ozaki, A., and Aika, K., "Catalysis, Science and Technology," Part 1, Chap. 3. Springer-Verlag, Berlin, 1981.
3. Ertl, G., Weiss, M., and Lee, S. B., *Chem. Phys. Lett.* **60**, 391 (1979).
4. Paal, Z., Ertl, G., and Lee, S. B., *Appl. Surf. Sci.* **8**, 231 (1981).
5. Nielsen, A., *Catal. Rev.* **4**, 1 (1970).

6. Frankenburg, W. G., in "Catalysis" (P. H. Emmett, Ed.), Vol. 3, p. 171. Reinhold, New York, 1955.
7. Ertl, G., in "Robert Welch Conferences on Chemical Research: XXV. Heterogeneous Catalysis," p. 179. Houston, 1981.
8. Spencer, N. D., Schoonmaker, R. C., and Somorjai, G. A., *J. Catal.* **74**, 129 (1982).
9. Strongin, D. R., Carrazza, J., Bare, S. R., and Somorjai, G. A., *J. Catal.* **103**, 213 (1987).
10. Madden, H. H., and Goodman, D. W., *Surf. Sci.* **150**, 39 (1985).
11. Emmett, P. H., in "The Physical Basis for Heterogeneous Catalysis" (E. Drouglis and R. I. Jaffee, Eds.), p. 3. Plenum, New York, 1975.
12. Biberian, J. P., and Somorjai, G. A., *Appl. Surf. Sci.* **2**, 352 (1979).
13. Wagner, C. D., in "Practical Surface Analysis" (D. Briggs and M. P. Seah, Eds.), Appendix 4. Wiley, New York, 1983.
14. Ertl, G., and Wandelt, K., *Surf. Sci.* **50**, 479 (1975).
15. Bare, S. R., Strongin, D. R., and Somorjai, G. A., *J. Phys. Chem.* **90**, 4726 (1986).
16. Grunze, M., Bozso, F., Ertl, G., and Weiss, M., *Appl. Surf. Sci.* **1**, 241 (1978).
17. Weiss, M., Ertl, G., and Nitschke, F., *Appl. Surf. Sci.* **2**, 614 (1979).
18. Dumesic, J. A., Topsoe, H., and Boudart, M., *J. Catal.* **37**, 513 (1975).
19. Langell, M., and Somorjai, G. A., *J. Vac. Sci. Technol.* **21**, 858 (1982).
20. Brundle, C. R., *Surf. Sci.* **66**, 581 (1977).
21. Overbury, S. H., Bertrand, P. A., and Somorjai, G. A., *Chem. Rev.* **75**(5), 547 (1975).
22. Beruto, D., Baro, L., and Passerone, A., in "Oxides and Oxide Films" (A. K. Vijn, Ed.), Vol. 6. Dekker, New York, 1981.
23. Sushumna, I., and Ruckenstein, E., *J. Catal.* **94**, 239 (1985).
24. Paparazzo, E., Dormann, J. L., and Fiorani, D., *Phys. Rev. B.* **28**, 1154 (1983).
25. Paparazzo, E., *Appl. Surf. Sci.* **25**, 1 (1986).
26. Borghard, W. S., and Boudart, M., *J. Catal.* **80**, 194 (1983).
27. Ludwiczek, H., Preisinger, A., Fischer, A., Hosemann, R., Schonfeld, A., and Vogel, W., *J. Catal.* **51**, 326 (1978).
28. Fagherazzi, G., Galante, F., Garbassi, F., and Pernicone, N., *J. Catal.* **26**, 344 (1972).
29. Khammouma, S., Ph.D. dissertation, Stanford University, 1972.